Open Access **Baghdad Science Journal** **P-ISSN: 2078-8665**
Published Online First: April 2021 **2021, 18(4): 1294-1302** **E-ISSN: 2411-7986**

DOI: http://dx.doi.org/10.21123/bsj.2021.18.4.1294

Using Fuzzy Clustering to Detect the Tumor Area in Stomach Medical Images

Ekhlas Falih Naser [*] ***Suhiar Mohammed Zeki***

Department of Computer Sciences, University of Technology, Baghdad, Iraq
[*]Corresponding author: 110022@uotechnology.edu.iq[*], 110121@uotechnology.edu.iq
[*]ORCID ID: https://orcid.org/0000-0002-6543-7751 [*], https://orcid.org/0000-0001-8337-4013

Received 14/1/2020, Accepted 13/7/2020, Published Online First 30/4/2021, Published 1/12/2021

Abstract:

Although the number of stomach tumor patients reduced obviously during last decades in western countries, but this illness is still one of the main causes of death in developing countries. The aim of this research is to detect the area of a tumor in a stomach images based on fuzzy clustering. The proposed methodology consists of three stages. The stomach images are divided into four quarters and then features elicited from each quarter in the first stage by utilizing seven moments invariant. Fuzzy C-Mean clustering (FCM) was employed in the second stage for each quarter to collect the features of each quarter into clusters. Manhattan distance was calculated in the third stage among all clusters' centers in all quarters to disclosure of the quarter that contains a tumor based on the centroid value of the cluster in this quarter, which is far from the centers of the remaining quarters. From the calculations conducted on several images' quarters, the experimental outcomes show that the centroid value of the cluster in each quarter was greater than 0.9 if this quarter did not contain a tumor while the value of the centroid value for the cluster containing a tumor was less than 0.4.For examples, in a quarter no.1 for STOMACH_1 medical image, the centroid value of the cluster was 0.973 while the value of the cluster centroid in quarter no.3 was 0.280. For this reason the tumor area was found in quarter no.(3) of the medical image STOMACH_1. Also, the centroid value of the cluster in a quarter no.2 was 0.948 for STOMACH_2 while, the value of the cluster centroid in quarter no.4 was 0.397. For this reason the tumor area was found in a quarter no.4 of the medical image STOMACH_2.

Keywords: FCM, Manhattan distance, Seven Moments, Stomach, Tumor.

Introduction:

The stomach is a segment of the gastrointestinal (GI) tract which receives food from the esophagus, mixes it, breaks it down, and then passes it on to the small intestine in smaller portions. In the stomach, the main secretory functions and digestion process begin. However, the most critical and important function of the stomach in digestive physiology is perhaps gastric motility. In this way, the functions of the stomach are mainly three: (i) the storage of large quantities of food to be further processed in the duodenum, and lower intestinal tract, (ii) the mixing of this food with gastric secretions to form a semi-fluid mixture, and (iii) to slow down the emptying of that semi-fluid mixture into the small intestine at a rate suitable for proper digestion and absorption. Regarding the motor activity, the stomach must consume glucose to generate the power necessary to carry out the digestion process. Although glucose consumption in the stomach is relatively low, it can affect the glucose concentration in the bloodstream (1).

A stomach traditionally is regarded as hollow muscular sac which starts the second digestion phase. So far this view simply disregards the fact that it is the most sophisticated endocrine organ with unique biochemistry, physiology, microbiology and immunology. Whole ingested materials which include the nutrition have to negotiate first this organ and as such the stomach is arguably the most significant piece within the tract of GI. The single biological duty of gastric acid secretion not only starts the digestive operation but acts also as a first defense line against microbes transferred by food-borne. Ordinary gastric physiology and morphology may be disrupted via infection of Helicobacter pylori, the ultimate popular chronic bacterial infection in the world and the etiological factor for most gastric cancer and peptic ulcers (2). Cancer is one of the ultimate

significant concerns in the life of people. It has the highest death average after the diseases of heart. Also, it has high death average psychological-economic and impairment results which rise due to the delay in diagnosis and accurate treatment. In accordance to the statistics introduced via The Organization of World Health , the cancer of stomach is the second widespread cancer in the world. As 50% of this cancer is inoperable and with available treatments there is no opportunity for more than 5 years life for the sufferers (3). A stomach is both an ingested food reservoir and a mixing and digestion chamber. It continues the procedure of chemical and mechanical digestion within the assistance of a group of gastric enzymes and its different smooth muscles layers, before funneling food turned into chyme into the duodenum. The stomach exists in the upper left quadrant of the abdomen and it is a J-shaped organ consists predominantly of involuntary smooth muscle. A food bolus enters the stomach via the lower oesophageal sphincter that quickly closes to prevent regurgitation of secretions' gastric (4).

There are four main regions in the stomach:

1) The cardia (or cardiac region) is the point where the esophagus connects to the stomach and through which food passes into the stomach.
2) Located inferior to the diaphragm, above and to the left of the cardia, is the dome-shaped fundus.
3) Below the fundus is the body, the main part of the stomach.
4) The funnel-shaped pylorus connects the stomach to the duodenum.

The wider end of the funnel, the pyloric antrum, connects to the body of the stomach. The narrower end is called the pyloric canal, which connects to the duodenum. The smooth muscle pyloric sphincter is located at this latter point of connection and controls stomach emptying. In the absence of food, the stomach deflates inward, and its mucosa and sub-mucosa fall into a large fold called a ruga. The addition of an inner oblique smooth muscle layer gives the muscularis the ability to vigorously churn and mix food. The convex lateral surface of the stomach is called the greater curvature; the concave medial border is the lesser curvature. The stomach is held in place by the lesser omentum, which extends from the liver to the lesser curvature, and the greater omentum, which runs from the greater curvature to the posterior abdominal wall (5). Figure 1 illustrates the stomach regions, the cardia, fundus, body, and pylorus.

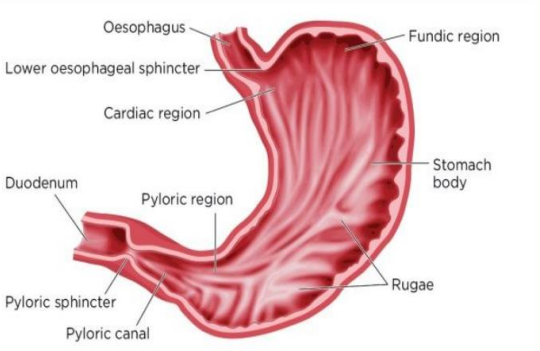

Figure 1. The main regions of the stomach (4)

Related Works

Various approaches for segmentation a tumor in a brain and diagnosis of cancer in a stomach were found. For example**,** by using image processing and artificial intelligence algorithms like primary preprocessors for increasing the quality and statistical characteristics of image, local binary pattern algorithm for elicit characteristics, image histogram algorithm to elicit impaired characteristics and support vector machine were used for accurate classification among impaired and suspected subjects and also for accurate diagnosis of impairment (6).Also, there was the application of two widely used algorithms for tumor detection (i) K-means clustering (ii) Fuzzy C Means clustering. The segmentation algorithms are compared to estimate the efficiency by evaluating the execution time and accuracy of the algorithm (7). The results of the proposed methodology show that the execution time was less in K-Means compared to Fuzzy C-Means clustering method in the process of detecting a quarter that contains a tumor, but the accuracy of the detection was low while the method of fuzzy C-Means method took a long time in the detection process but with high accuracy.

Proposed Methodology

The proposed methodology for detection tumor area in the stomach medical magnetic resonance imaging (MRI) images has three stages. The stomach images are divided into 4 quarters. When the image is divided into 8 or 16 quarters, the results of determining the area that containing the tumor do not change, but rather the number of clusters increases, and therefore requires more time to calculate the seven moments of discharge and more time to calculate the value of the fuzzy of each cluster and the tumor may be distributed over two or more quarters, so for ease of calculation and with the least time and determining only one quarter containing the tumor, the image is divided into four quarters only.

The stomach images are divided into four quarters and then features elicited from each quarter in the first stage by utilizing seven moments invariant. Fuzzy C-Mean clustering (FCM) was employed in the second stage for each quarter to collect the features of each quarter into clusters. Manhattan distance was calculated in the third stage among all clusters' centers in all quarters to detect the value of center that far away from other centers and determine quarter that contains tumor based on the center's value. The block diagram of the proposed methodology is illustrated in Fig.2.

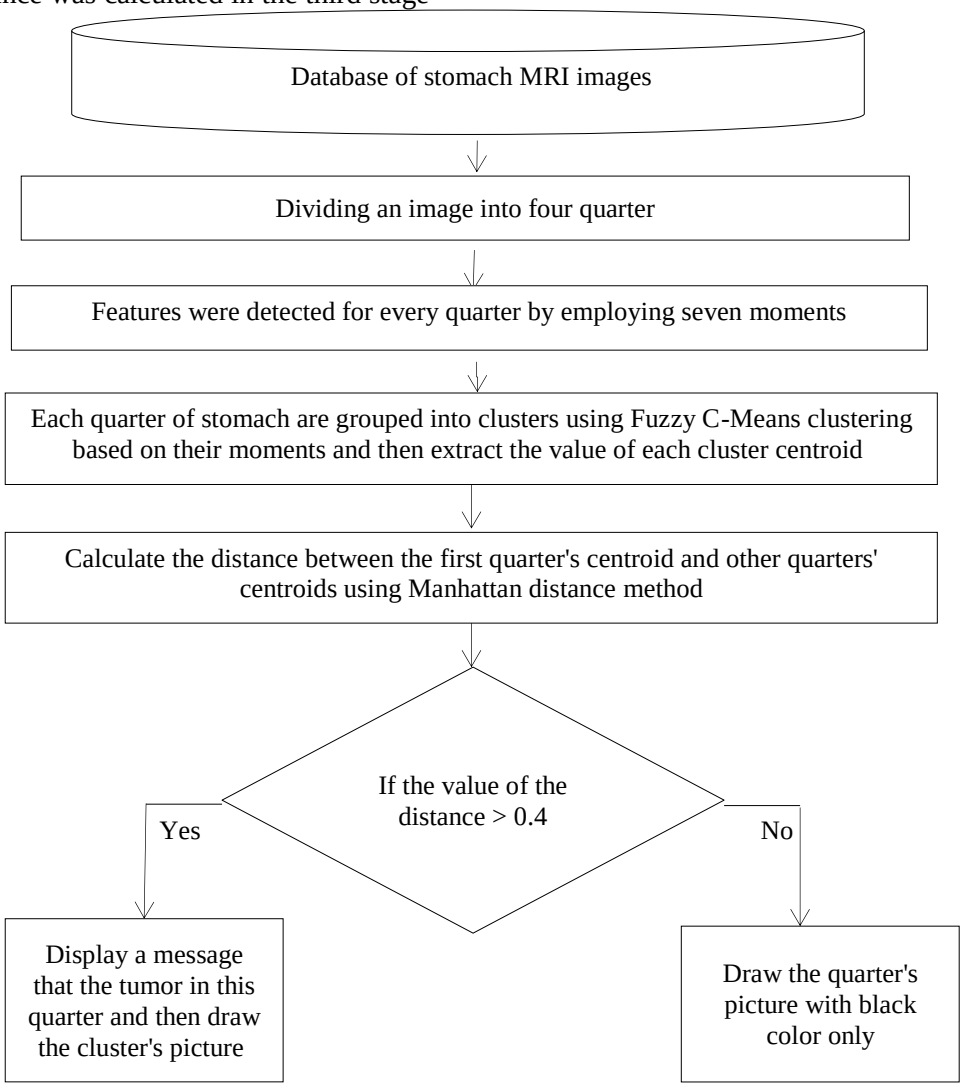

Figure 2. A Block diagram of the Proposed Methodology for Detection

Features Extraction Using Seven Moments Invariants

This approach has been widely used to image pattern recognition in a variety of applications because of their unchanged features on picture rotation, scaling, and translation. Moment invariants are helpful for calculating sets of region characteristics that can be utilized for shape recognition. Suppose (F (x, y)) defined a 2 dimension array of numbers in a spatial model. A Geometric moment of arrangement *(p + q)* is illustrated in Eq.1 (8).

$$m_{p,q} = \sum_{x} \sum_{y} x^p y^q F(x,y) \qquad (1)$$

F(x,y) represents the values of image's pixels for(p , q = 0 , 1 , 2 , ...).The central of moments are defined via Eq.2 (8).

$$x_c = m_{1,0} / m_{0,0}$$
$$y_c = m_{0,1} / m_{0,0} \qquad (2)$$

Where x_c and y_c offers at Eq. 2 defined the region's center of an object. The moments that have the feature of translation unchanged are called central moments and are referred by $\mu_{p,q}$. It can be simplify confirmed that the central moments up to the order p+q≤3, may be calculated by the Eq.3 (8).

$$\left.\begin{aligned}
\mu_{0,0} &= m_{0.0} \\
\mu_{1,0} &= 0 \\
\mu_{0,1} &= 0 \\
\mu_{2,0} &= m_{2,0} - x_c m_{1,0} \\
\mu_{0,2} &= m_{0,2} - y_c m_{0,1} \\
\mu_{1,1} &= m_{1,1} - y_c m_{1,0} \\
\mu_{3,0} &= m_{3,0} - 3x_c m_{2,0} + 2m_{1,0} {x_c}^2 \\
\mu_{1,2} &= m_{1,2} - y_c m_{1,1} - x_c m_{0,2} + 2{y_c}^2 m_{1,0} \\
\mu_{2,1} &= m_{2,1} - 2x_c m_{1,1} - y_c m_{2,0} + 2{x_c}^2 m_{0,1} \\
\mu_{0,3} &= m_{0,3} - 3y_c m_{0,2} + 2{y_c}^2 m_{0,1}
\end{aligned}\right\} \quad (3)$$

Unchanged scale could be obtained by utilizing normalized central moments. An important step for feature extraction is feature normalization. Complex image database use features that are generated by many different feature extraction algorithms with different kinds of sources. These feature vectors usually exist in a very high dimensional space. Not all of these features have the same range. The applied normalization process maps the extracted feature values to the range between [0, 1].

The normalized central moments; indicate $\eta_{p,q}$ as illustrated in Eq.4 (6).

$$\eta_{p,q} = \mu_{p,q} / \mu^{\gamma}{}_{0,0} \quad (4)$$

Where $\gamma = p + q/2$

For Eq.4, (p + q = 2 , 3 ,…,p*q) . A seven non-linear absolute moment invariants, computed from normalizing central moments through order three are gotten in Eq.5 (8).

$$\left.\begin{aligned}
\phi 1 &= \eta_{2,0} + \eta_{0,2} \\
\phi 2 &= (\eta_{2,0} + \eta_{0,2})^2 + 4\eta_{1,1} \\
\phi 3 &= (\eta_{3,0} - 3\eta_{1,2})^2 + (3\eta_{2,1} - \eta_{0,3})^2 \\
\phi 4 &= (\eta_{3,0} + 3\eta_{1,2})^2 + (3\eta_{2,1} + \eta_{0,3})^2 \\
\phi 5 &= (\eta_{3,0} - 3\eta_{1,2})(\eta_{3,0} + 3\eta_{1,2})[(\eta_{3,0} + 3\eta_{1,2})^2 \\
&\quad - 3(\eta_{2,1} + \eta_{0,3})^2] + (3\eta_{2,1} - \eta_{0,3})(\eta_{2,1} + \eta_{0,3}) \\
&\quad [3(\eta_{3,0} + \eta_{1,2})^2 - (\eta_{2,1} + \eta_{0,3})^2] \\
\phi 6 &= (\eta_{2,0} + \eta_{0,2})[(\eta_{3,0} + \eta_{1,2})^2 - (\eta_{2,1} - \eta_{0,3})^2] \\
&\quad + 4\eta_{1,1}(\eta_{3,0} + \eta_{1,2})(\eta_{2,1} - \eta_{0,3}) \\
\phi 7 &= (3\eta_{2,1} - \eta_{0,3})(\eta_{3,0} + \eta_{1,2})[(\eta_{3,0} + \eta_{1,2})^2 \\
&\quad - 3(\eta_{2,1} + \eta_{0,3})^2] + (3\eta_{1,2} - \eta_{3,0})(\eta_{2,1} + \eta_{0,3}) \\
&\quad [3(\eta_{3,0} + \eta_{1,2})^2 - (\eta_{2,1} - \eta_{0,3})^2]
\end{aligned}\right\} \quad (5)$$

This group of normalized central moments is constant to rotation, translation and scale alterations for an image (8).

FCM

Fuzzy clustering is a strong unsupervised technique to data analysis and modes building. Objects on the boundaries between several classes are not forced to fully belong to one of the classes, but rather are assigned membership degrees between 0 and 1 indicating their partial membership. Clustering algorithm of FCM is one of the widely employed techniques between associated fuzzy models. Fuzzy clustering techniques can be employed to count the function of membership which defines to which degree the objects belong to clusters and employed to detect the overlapping

clusters in the data-set. The FCM utilizes fuzzy partitioning such that a data point can belong to all groups with different membership grades between 1 and 0 (9). This algorithm can work by specifying membership for every data-point that corresponds with every center of cluster based on the basis of distance among the center of data point and a cluster. Further data is near to a center of the cluster further is its membership across a specific center of the cluster. The addition from membership for every data point must be equal to one. This algorithm specifies a membership value to the items of the data for the clusters within a scope of 1 to 0. Thus an amount of fuzzy sets of partial membership can be incorporated and forms overlapping clusters for supporting it (10). This algorithm requires an argument known a fuzzification (m) which has a domain [1, *n*]. This fuzzification argument employed to determine the fuzziness's degree in these clusters. As the amount of (m) equals 1 this very algorithm works as if it is a crisp portioning algorithm and the clusters' overlapping tend to be more for larger amounts of (m) (11). The algorithm computes the value of a membership via utilized Eq.6 (11).

$$\mu_j(X_i) = \frac{\left(\frac{1}{d_{ji}}\right)^{\frac{1}{m-1}}}{\sum_{k=1}^{P}\left(\frac{1}{d_{ki}}\right)^{\frac{1}{m-1}}} \qquad (6)$$

where , ($\mu_j(X_i)$)is the membership of (X_i) in the cluster's (j^{th}) , (d_{ji}) is the distance of (X_i) in the cluster (C_i) , (m) is the parameter of fuzzification , (p) is the number of specified cluster , and (d_{ki}) is the distance of (X_i) in the cluster (C_k). The latest cluster enters are computed with a value of memebership via employing Eq.7 (11).

$$\sum_{j=1}^{p} \mu_j\ (x_i) = 1 \qquad (7)$$

Employing Eq.(7) to compute the latest values of the membership is done and is computed by employing Eq.8 (11).

$$C_j = \frac{\sum_i [\mu_j(x_i)]^m x_i}{\sum_i [\mu_j(x_i)]^m} \qquad (8)$$

Where, (C_j) is the center of (j^{th}) cluster , (x_i) is i^{th} data point , (m) is the parameter of the fuzzification and (μ_j) is the function that retrun the membership.The weighted average's form can be computed via utilizing this form specially. The fuzziness's degree in (x_i 's) current membership can be computed and this is multiplied by (x_i) (11).

Sum of the fuzzified membership divides the product acquired. Recent centroids are computed in this style**.**After clustering the seven moments in each cluster, the Manhattan for those features can be calculated via Eq. 9. The Manhattan distance between two components can be calculated by the summation of differences of their identical elements. The distance formula among the points A= (a1, a2, etc.) within the points B= (b1, b2, etc.) can be calculated via Eq.9 (12).

$$d = \sum_{i=0}^{n} |a_i - b_i| \qquad (9)$$

Suggested Algorithm

A suggested algorithm can be offered like:

Algorithm 1. illustrates a suggested methodology main steps

Input: - Images of medical stomach
Output: - Detect the location of quarter that contains tumor

Begin
Step-1: **For** k=1 to count of images.
Step-2: acquire **Imags[k]** and divide **Imags[k**] into four quarter
Step-3: For each quarter **do**
Step-3-1: Feature are detected for **all (Images[k])** by employing seven moments invariant and save the outcomes in **(SM_Imags[k])**
Step-3-2: Apply Fuzzy clustering algorithm to each quarter and save the outcomes in **(SMF_Imags[k])**.
End //for each quarter
Step-4: Apply Manhattan distance among the centers of clusters using Eq 9 to determine the faraway center.
Step-5: Disclosure of the quarter that contains a tumor based on the coordinates of the center of this quarter, which is far from the centers of the remaining quarters.
End // for loop for k
End.

Empirical Outcomes

The empirical outcomes of an offered methodology would be explained and offered in this section. C# language is utilized to implement the suggested method. Numbers of stomach medical images of type MRI in a database are 30 images. MRI used in the proposed methodology due to the fact that this type of image is distinguished as it deals with soft tissues , displays images with more details of the segment to be diagnosed within the body and is also capable of imaging in multiple axes and highlighting angles

Images in the database are colored Joint photo Graphic Experts Group (JPEG) with size 200 × 200 pixels. The size of the MRI images has been standardized in the proposed system, which are 200 pixels in length and 200 pixels in width for easy handling

The proposed methodology involves multiple stages:-

1) A process of loading the images of medical stomach onto the project's form can be carried out in the headmost stage as explained in Fig. 3.

The stomach images are divided into four quarters rather than divided into 8 or 16

Baghdad Science Journal
2021, 18(4): 1294-1302
P-ISSN: 2078-8665
E-ISSN: 2411-7986

quarters for the ease of calculation and with the least time and determining only one quarter containing the tumor, the image is divided into four quarters only. Dividing the images into four quarters as explained in Fig.4 for **STOMACH_1** and Fig.5 for **STOMACH_2**.

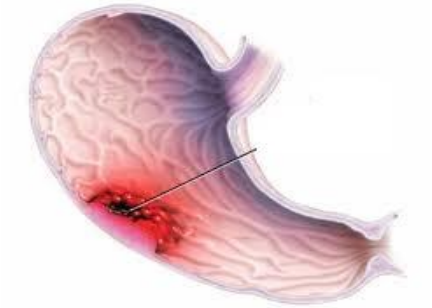

a)

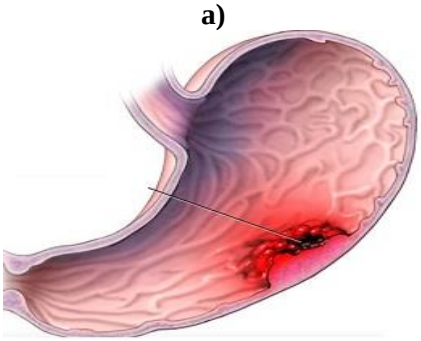

b)

Figure 3. Stomach images, a) STOMACH_1.JPG,b) STOMACH_2.JPG

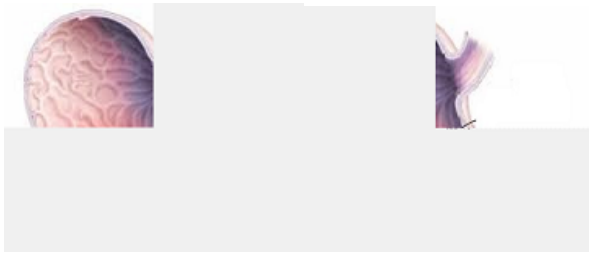

a) **b)**

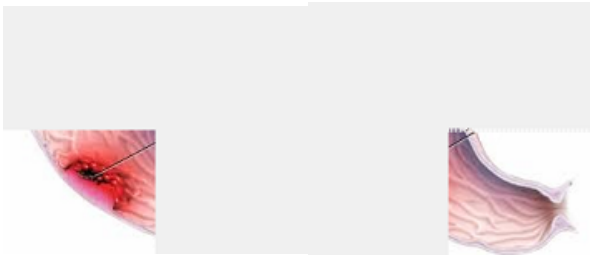

c) **d)**

Figure 4. Quarters sub-images of STOMACH_1, a) first quarter, b) second quarter, c) third quarter and d) fourth quarter

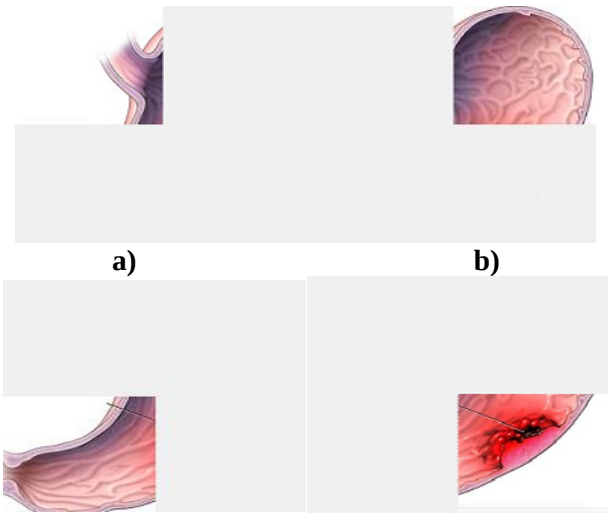

a) **b)**

c) **d)**

Figure 5. Quarters sub-images of STOMACH_2, a) first quarter, b) second quarter, c) third quarter and d) fourth quarter

Seven moments invariant for each quarter are calculated as illustrated in Table 1. The variable M1 indicates Moment 1, the variable M2 indicates moment 2, the variable M3 indicates moment, the variable M4 indicates moment 4,the variable M5 indicates moment 5,the variable M6 indicates moment 6 and the variable M7 indicates moment 7.

Table 1. displays the values of the seven moments invariant for each quarter

Image Name	Quarter No.	M1	M2	M3	M4	M5	M6	M7
	Quarter_1	8.327	5.062	1.953	1.930	8.631	3.388	7.151
Somach_1	Quarter_2	3.232	7.399	1.529	1.511	5.982	1.144	5.587
	Quarter_3	-5.253	-1.597	-6.659	-6.620	-5.434	-4.997	-1.716
	Quarter_4	1.945	1.099	1.546	1.523	1.922	2.395	2.639
	Quarter_1	8.527	6.180	8.829	8.811	2.623	1.882	1.077
Somach_2	Quarter_2	1.371	9.967	8.611	8.603	4.219	4.316	3.610
	Quarter_3	1.342	9.614	8.973	8.936	8.500	4.460	6.484
	Quarter_4	-1.146	-7.259	-2.238	-2.213	-3.349	-6.565	-1.384

2) In the second step, the fuzzy C-Means clustering was applied to each quarter using the C-Means clustering method as illustrated in Fig.6 for stomach_1 and Fig.7 for stomach_2.

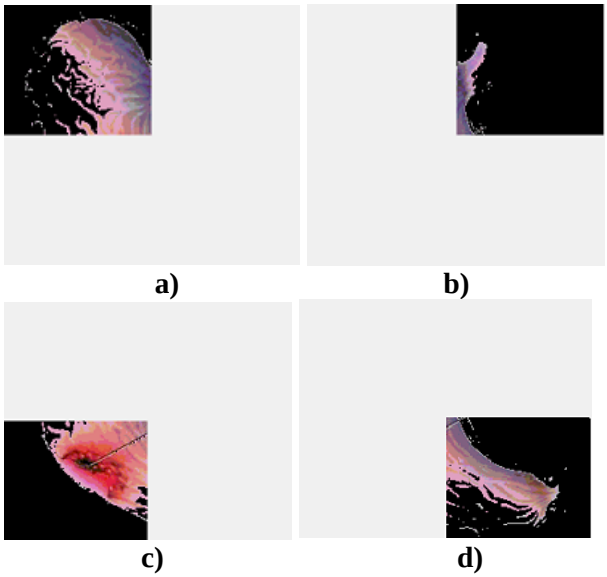

a) b) c) d)

Figure 6. Clusters of quarters of STOMACH_1 a) first quarter, b) second quarter, c) third quarter and d) fourth quarter

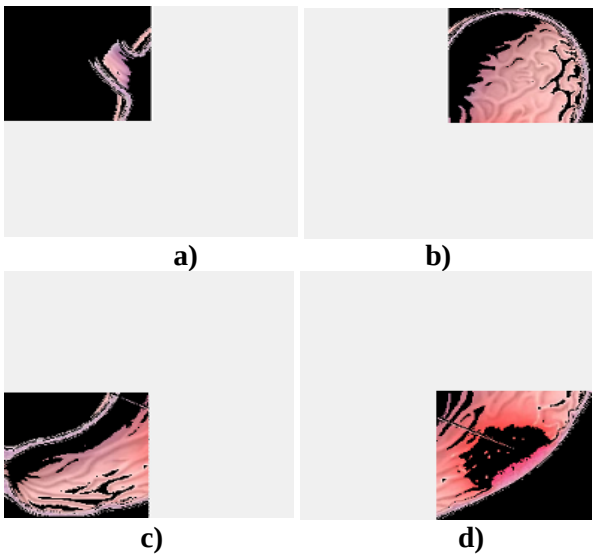

a) b) c) d)

Figure 7. Clusters of quarters of STOMACH_2 a) first quarter, b) second quarter, c) third quarter and d) fourth quarter

3) Employing Manhattan distance to detect of the quarter that contains a tumor based on the value of the center of this quarter, which is far from the centers of the remaining quarters as displayed in Table 2. Figure 8 and 9 illustrate the detection process.

Figure 8. Detection the tumor's location in a STOMACH_1

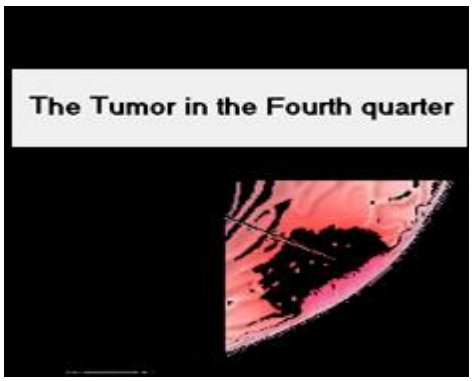

Figure 9. Detection the tumor's location in a in STOMACH_2

Table 2. shows the values of the cluster centroid of each quarter for two samples of stomach images (STOMACH_1 and STOMACH_2).

Image Name	Quarter No.	Cluster's Centroids
STOMACH_1	Quarter No._1	0.973
	Quarter No._2	0.998
	Quarter No._3	0.280
	Quarter No._4	0.985
STOMACH_2	Quarter No._1	0.968
	Quarter No._2	0.948
	Quarter No._3	0.994
	Quarter No._4	0.397

Table 3 shows the comparison for tumor detection between K-Means clustering method and fuzzy C-Means clustering method in term of time consuming and accuracy. From Table (3), it becomes clear to us that K-Menes method took a little time in the process of detecting a quarter that contains a tumor, but the accuracy of the detection was low while the fuzzy C-Means method took a long time in the detection process but with high accuracy.

The performance of the proposed methodology can be calculated based on accuracy. Accuracy is calculated by the measures of

sensitivity and specificity (13). It is denoted as in Eq.10. (13)

$$\text{Accuracy} = \frac{TP+TN}{TP+TN+FP+FN} \text{ x100} \quad (10)$$

Where TP displays true positives predication, TN displays true negative predication, FP displays false positives predication and FN displays false negative predication (13).

Table 3. shows the comparison for tumor detection between K-Means clustering method and fuzzy clustering method in term of time consuming and accuracy.

Method Name	Object name	Time(sec) for detection	Accuracy for detection
K-Means Clustering	STOMACH_1	0.0527	73%
	STOMACH_2	0.0783	69%
Fuzzy Clustering	STOMACH_1	1.531	85%
	STOMACH_2	1.9930	83%

Conclusions:

The aim of this research is to detect the area of a tumor in a stomach images based on fuzzy clustering. A methodology utilized seven moments invariant to elicit the features of the stomach medical image which is simpler and easer to calculate. Utilizing the invariant ability to the affine transformations of features for handle various input conditions. FCM is really convenient to handle the affair concerning for understanding pattern capability, noise and incomplete data, mixed information of media, interaction of human and it supply the solutions quickly. The Manhattan distance is based on absolute value distance, as opposed to Euclidean distance. Absolute value distance should give more robust results, whereas Euclidean would be influenced by unusual value. From the calculations conducted on several quarters of images, the experimental outcomes show that the centroid value of the cluster in each quarter was greater than 0.9 if this quarter did not contain a tumor while the value of the centroid value for the cluster that containing a tumor was less than 0.4. Form Table 2 in the quarter no.1 for STOMACH_1 medical image, the centroid value of the cluster was 0.973 while the value of the cluster centroid in quarter no.3 was 0.280. For this reason the tumor area was found in quarter no.(3) of the medical image STOMACH_1. Also, the centroid value of the cluster in a quarter no.2 was 0.948 for STOMACH_2 while, the value of the cluster centroid in quarter no.4 was 0.397. For this reason the tumor area was found in a quarter no.4 of the medical image STOMACH_2.

Authors' declaration:

- Conflicts of Interest: None.
- We hereby confirm that all the Figures and Tables in the manuscript are mine ours. Besides, the Figures and images, which are not mine ours, have been given the permission for re-publication attached with the manuscript.
- Ethical Clearance: The project was approved by the local ethical committee in University of Technology.

References

1. Lema-Perez L, Garcia-Tirado J, Builes-Montaño C, Alvarez H. Phenomenological-Based model of human stomach and its role in glucose metabolism. J. Theor. Biol.2019 Jan 7;460:88-100.
2. Etemadi A, Safiri S, Sepanlou SG, Ikuta K, Bisignano C, Shakeri R, et al. The global, regional, and national burden of stomach cancer in 195 countries, 1990–2017: a systematic analysis for the Global Burden of Disease study 2017. Lancet Gastroenterol. Hepatol. 2020 Jan 1;5(1):42-54.
3. Lai Z, Deng H. Medical Image Classification Based on Deep Features Extracted by Deep Model and Statistic Feature Fusion with Multilayer Perceptron.Comput.Intell.NeurScien.2018 Sep. 12; 2018.
4. Knight J, Williams N, Nigam Y. Gastrointestinal tract 2: the structure and function of the stomach. Nursing Times. 2019 Jul 1;115(7):43-7.
5. Mahadevan V. Anatomy of the stomach. Surgery (Oxford). 2014 Nov 1;32(11):571-4.
6. Ahmadzadeh D, Fiuzy M, Haddadnia J. Stomach cancer diagnosis by using a combination of image processing algorithms, local binary pattern algorithm and support vector machine. J. Basic. Appl. Sci. Res. 2013;3(2):43-51.
7. Nimeesha KM, Gowda RM. Brain tumour segmentation using Kmeans and fuzzy c-means clustering algorithm. Int J Compute Sci Inform. Techno. Res. Excell. 2013 Mar;3:60-5.
8. Mustafa RA, Saleh KT, Chyad HS. Feature Extraction Based on Wavelet Transform and Moment Invariants for Medical Image. IJERAT. 2018Aug: 4(8): 80-98.
9. Xu J, Han J, Nie F, Li X. Robust and Efficient Fuzzy C-Means Clustering Constrained on Flexible Sparsity. arXiv preprint arXiv:1908.06699. 2019 Aug 19.
10. Gokten PO, Baser F, Gokten S. Using fuzzy c-means clustering algorithm in financial health scoring. The Audi. Finan. J. 2017;15(147):385-394.
11. Joan M, Nuñez DR, Carles VR. Fuzzy C-means and clustering algorithms: a comparative study. Grau en Eng. Inform. Intel. Artifi. .2019 Jun : 17-20.
12. Karim AA, Nasser EF. Image Retrieval from Video Streams Databases using Similarity of Clustering Histogram. Al-Mans. J. .2018(29):1-22.

13. Bramarambika MB , Seshashayee. Brain Tumor Detection and Identification Using Histogram Method. IJITEE. 2019 Aug: 8 (10):3517-3521.

استخدام التجميع الضبابي للكشف عن منطقة الورم في صور المعدة الطبية

أخلاص فالح ناصر **سهير محمد زكي**

قسم علوم الحاسوب، الجامعه التكنولوجيه، بغداد، العراق

الخلاصة:

على الرغم من انخفاض عدد المرضى المصابين بورم في المعدة بشكل واضح خلال العقود الماضية في الدول الغربية ، إلا أن هذا المرض لا يزال أحد الأسباب الرئيسية للوفاة في البلدان النامية. الهدف من هذا البحث هو اكتشاف منطقة الورم في صور المعدة بالأعتماد على التجميع الضبابي. تتكون الطريقه المقترحة من ثلاث مراحل. تنقسم صور المعدة إلى أربعة أرباع ، ثم يتم استنباط صفات كل ربع في المرحلة الأولى من خلال أستخدام العزوم الثابته السبعه . في المرحله الثانيه تم أستخدام التجميع الضبابي (FCM) وذلك لجمع صفات كل ربع في مجاميع (clusters). تم حساب مسافة مانهاتن في المرحلة الثالثة بين جميع مراكز التجمعات (clusters)في جميع الأرباع للكشف عن الربع الذي يحتوي على ورم والذي يعتمد على قيمة النقطه الوسطى للكتله في هذا الربع ، وهوالذي تكون أحداثياته بعيده عن إحداثيات مراكز الأرباع المتبقية. من الحسابات التي أجريت على أرباع عدة صور ، أظهرت النتائج التجريبية أن قيمة النقطه الوسطى للكتلة في كل ربع سنة كانت أكبر من 0.9 إذا لم يكن هذا الربع يحتوي على ورم بينما كانت قيمة النقطه الوسطى للكتلة التي تحتوي على ورم أقل من 0.4. على سبيل المثال ، في الربع رقم 1 للصورة الطبية STOMACH_1 ، كانت قيمة النقطة المركزية للكتلة 0.973 بينما كانت قيمة النقطة المركزية للكتلة في الربع الثالث 0.280. لهذا السبب تم العثور على منطقة الورم في الربع رقم (3) من الصورة الطبية STOMACH_1. أيضا ، كانت قيمة النقطة المركزية للكتلة في الربع رقم 2 0.948 لـ STOMACH_2 بينما كانت قيمة النقطة المركزية للكتلة في الربع رقم 4 0.397. لهذا السبب تم العثور على منطقة الورم في الربع رقم 4 من الصورة الطبية STOMACH_2.

الكلمات المفتاحيه: التجميع الضبابي (FCM) ، مسافة منهاتن ، العزوم السبعه ، المعده ، الورم.